Region Matching with Missing Parts[*]

Alessandro Duci[1,4], Anthony J. Yezzi[2], Sanjoy Mitter[3], and Stefano Soatto[4]

[1] Scuola Normale Superiore, Pisa – Italy 56100
`alessandro.duci@sns.it`
[2] Georgia Institute of Technology, Atlanta – GA 30332
`ayezzi@ece.gatech.edu`
[3] Massachusetts Institute of Technology, Cambridge – MA 02139
`mitter@lids.mit.edu`
[4] University of California at Los Angeles, Los Angeles – CA 90095
`soatto@ucla.edu`

Abstract. We present a variational approach to the problem of registering planar shapes despite missing parts. Registration is achieved through the evolution of a partial differential equation that simultaneously estimates the shape of the missing region, the underlying "complete shape" and the collection of group elements (Euclidean or affine) corresponding to the registration. Our technique applies both to shapes, for instance represented as characteristic functions (binary images), and to grayscale images, where all intensity levels evolve simultaneously in a partial differential equation. It can therefore be used to perform "region inpainting" and to register collections of images despite occlusions. The novelty of the approach lies on the fact that, rather than estimating the missing region in each image independently, we pose the problem as a joint registration with respect to an underlying "complete shape" from which the complete version of the original data is obtained via a group action.

Keywords: shape, variational, registration, missing part, inpainting

1 Introduction

Consider different images of the same scene, taken for instance from a moving camera, where one or more of the images have been corrupted, so that an entire part is missing. This problem arises, for instance, in image registration with missing data, in the presence of occlusions, in shape recognition when one or more parts of an object may be absent in each view, and in "movie inpainting" where one or more frames are damaged and one wants to "transfer" adjacent frames to fill in the damaged part.

We consider a simplified version of the problem, where we have a compact region in each image i, bounded by a closed planar contour, γ_i, and a region of the image, with support described by a characteristic function χ_i, is damaged. We do not know a-priori what the region χ_i is, and we do not know the transformation

---

mapping one image onto the other. However, we make the assumption that such a transformation can be well approximated by a finite-dimensional group g_i, for instance the affine or the projective group. In addition, we do not know the value of the image in the missing region. Therefore, given a sequence of images, one has to simultaneously infer the missing regions χ_i as well as the transformations g_i and the occluded portions of each contour γ_i.

We propose an algorithm that stems from a simple generative model, where an unknown contour μ_0, the "complete shape," is first transformed by a group action g_i, and then occluded by a region χ_i (Figure 1). Therefore, one only estimates the complete shape and the group actions:

$$\hat{g}_1, \ldots, \hat{g}_k, \hat{\mu}_0, \hat{\chi}_1, \ldots, \hat{\chi}_k = \arg\min_{g_i, \mu_0} \sum_{i=1}^{k} \phi(\chi_i(\gamma_i), \chi_i \circ g_i(\mu_0)) \qquad (1)$$

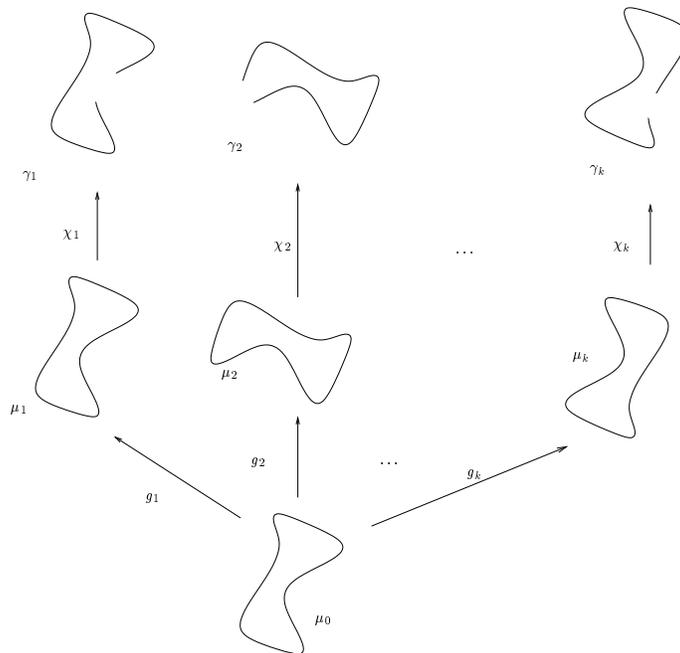for a given discrepancy measure ϕ. A simpler case is when the occlusion occurs at

Fig. 1. *A contour undergoes a global motion and local occlusions.*

the same location in all shapes; in this case, there is only one indicator function χ_0 that acts on the complete shape μ_0.

2 Background and prior work

The analysis of "Shape Spaces" was pioneered in Statistics by Kendall, Mardia and Carne among others [12, 17, 6, 20]. Shapes are defined as the equivalence classes of points modulo the similarity group, $\mathbb{R}^{MN}/SE(M) \times \mathbb{R}$. These tools have proven useful in contexts where N distinct "landmarks" are available, for instance in comparing biological shapes with N distinct "parts." Various extensions to missing points have been proposed, mostly using expectation-maximization (EM), alternating between computing the sufficient statistics of the missing data and performing shape analysis in the standard framework of shape spaces. However, since this framework is essentially tied to representing shapes as collections of points, they do not extend to the case of continuous curves and surfaces in a straightforward way, and we will therefore not pursue them further here.

In computational vision, a wide literature exists for the problem of "matching" or "aligning" discrete representations of collections of points, for instance organized in graphs or trees [16, 8]. A survey of shape matching algorithms is presented in [29]. Just to highlight some representative algorithms, Belongie et al. [2] propose comparing planar contours based on the "shape context" of each point along the contour. This work is positioned somewhere in between landmark or feature-based approaches and image-based ones, similarly to [7]. Kang et al. [11] have recently approached the multiple image inpainting problem using a shape context representation.

Deformable templates, pioneered by Grenander [9], do not rely on a point-wise representation; rather, images are deformed under the action of a group (possibly infinite-dimensional) and compared for the best match in an image-based approach [32, 3]. Grenander's work sparked a current that has been particularly successful in the analysis of medical images, for instance [10]. In this work we would like to retain some of the features of deformable templates, but extend them to modeling missing parts. A somewhat different line of work is based on variational methods and the solution of partial differential equations (PDEs) to deform planar contours and quantify their "distance." Not only can the notion of alignment or distance be made precise [1, 31, 21, 14, 26], but quite sophisticated theories of shape, that encompass perceptually relevant aspects, can be formalized in terms of the properties of the evolution of PDEs (e.g. [15, 13]). The variational framework has also been proven very effective in the analysis of medical images [19, 28, 18]. Zhu et al. [33] have also extended some of these ideas to a probabilistic context.

Other techniques rely on matching different representations, for instance skeletons [13], that are somewhat robust to missing parts. In [27] a similar approach is derived using a generic representation of 2-D shape in the form of structural descriptions from the shocks of a curve evolution process, acting on bounding contours.

The possibility of making multiple registration by finding a mean shape and a rigid transformation was studied by Pennec [24] in the case of 3D landmarks. Leung, Burl and Perona [5] described an algorithm for locating quasi-frontal

views of human faces in cluttered scenes that can handle partial occlusions. The algorithm is based on coupling a set of local feature detectors with a statistical model of the mutual distances between facial features.

In this work, we intend to extend these techniques to situations where parts of the image cannot be used for matching (see [30]) and at the same time landmark approaches fail. In the paper of Berger and Gerig [4], a deformable area-based template matching is applied to low contrast medical images. In particular, they use a least squares template matching (LSM) with an automatic quality control of the resulting match. Nastar, Moghaddam and Pentland [22] proposed to use a statistical learning method for image matching and interpolation of missing data. Their approach is based on the idea of modeling the image like a deformable intensity surface represented by a 3D mesh and use principal component analysis to provide a priori knowledge about object-specific deformations. Rangarajan, Chui and Mjolsness [25] defined a novel distance measure for non-rigid image matching where probabilistic generative models are constructed for the nonrigid matching of point-sets.

2.1 Contributions of this paper

This work presents a framework and an algorithm to match regions despite missing parts. To the best of our knowledge, work in this area, using region-based variational methods, is novel. Our framework relies on the notion of "complete shape" which is inferred simultaneously with the group actions that map the complete shape onto the incomplete ones. The complete shape and the registration parameters are defined as the ones that minimize a cost functional, and are computed using an alternating minimization approach where a partial differential equation is integrated using level set methods [23].

3 Matching with missing parts

The formulation of the problem and the derivation of the evolution equations are introduced in this section for the case of a planar shape under isometric transformations (rigid motions). In this case, the dimension of the space is 2 and the determinant of the Jacobian of the group is $J(g) = 1$ for all the elements g of the group G. The main assumption about the shape is that it must be a *regular domain*, that is an open and bounded subset of $\mathbb{R}^2$ with a finite number of connected components and a piece-wise C^∞ boundary. This regularity is required to avoid singular pathologies and to make the computation possible. The main notation that will be used in this section is listed below.
Notation

- $\bar{\gamma}_i, \bar{\mu}$ are regular domains in $\mathbb{R}^2$
- γ_i, μ are the boundaries of $\bar{\gamma}_i, \bar{\mu}$
- $\chi(\gamma)$ is the characteristic function of the set $\bar{\gamma}$
- $A(\gamma)$ is the area (volume) of the region $\bar{\gamma}$
- $\langle \cdot, \cdot \rangle$ is the usual inner product

3.1 Formulation of the problem

Let $\bar{\gamma}_1, \ldots, \bar{\gamma}_k$ be regular domains of $\mathbb{R}^2$, all obtained from the same regular domain $\bar{\mu} \subset \mathbb{R}^2$ by composition with characteristic functions

$$\chi_1, \ldots, \chi_k : \mathbb{R}^2 \to \mathbb{R}$$

and actions of Lie group elements $g_1, \ldots, g_k \in G$. We want to find the best solution in the sense expressed by the functional

$$\phi = \sum_{i=1}^{k} A(\bar{\gamma}_i \setminus g_i(\bar{\mu})) + \alpha \, A(\bar{\mu}) \tag{2}$$

where A denotes the area, α is a design constant, $\bar{\mu}$, χ_i and g_i are the unknowns and the sets $\bar{\gamma}_i$ and the structure of G are given. The rationale behind the choice of the cost function ϕ is that one wants to maximize the overlap between the incomplete shapes and the registered complete shape (first term) while keeping the complete shape as small as possible (second term). This is equivalent to minimizing the area of the $\bar{\gamma}_i$ that is not covered by the image of the complete shape after the application of the group action g_i. At the same time, one needs to minimize a quantity related to the complete shape (e.g. the area) to constrain the solution to be non-singular. Without the second term, it is always possible to choose a compact complete shape that covers all the incomplete ones (e.g. a big square) and minimizes the first term.

3.2 Minimization with respect to shape

The functional ϕ can be written in integral form

$$\phi = \sum_{i=1}^{k} \int_{\bar{\gamma}_i} (1 - g_i \bar{\mu}) d\mathbf{x} + \alpha \int_{\bar{\mu}} d\mathbf{x} \tag{3}$$

and using the characteristic function notation

$$\phi = \sum_{i=1}^{k} \int \chi(\gamma_i)(1 - \chi(g_i \mu)) d\mathbf{x} + \alpha \int \chi(\mu) d\mathbf{x} \tag{4}$$

$$= \sum_{i=1}^{k} \int \chi(\gamma_i) d\mathbf{x} - \sum_{i=1}^{k} \int \chi(\gamma_i) \chi(g_i \mu) d\mathbf{x} + \alpha \int \chi(\mu) d\mathbf{x}. \tag{5}$$

Since the first term of ϕ is independent of μ, g and remembering that g_i are isometries, the problem of minimizing ϕ is equivalent to that of finding the minimum of the energy

$$E(g_i, \mu) = \int_{\bar{\mu}} \left(\alpha - \sum_{i=1}^{k} \chi(g_i^{-1} \gamma_i) \right) d\mathbf{x}. \tag{6}$$

One can show that the first variation of this integral along the normal direction of the contour is simply its integrand, by using the divergence theorem, and therefore conclude that a gradient flow that minimizes the energy E with respect to the shape of the contour μ is given by

$$\frac{\partial \mu}{\partial t} = \left(\alpha - \sum_{i=1}^{k} \chi(g_i^{-1} \gamma_i) \right) N \tag{7}$$

where N is the normal vector field of the contour μ.

3.3   Minimization with respect to the group action

In order to compute the variation of the functional ϕ with respect to the group actions g_i, we first notice that there is only one term that depends on g_i in equation (6). Therefore, we are left with having to compute the variation of

$$-\int_{\bar{\mu}} \chi(g_i^{-1} \gamma_i) d\mathbf{x}. \tag{8}$$

In order to simplify the notation, we note that the term above is of the generic form

$$W(g) \doteq \int_{\bar{\mu}} f(g(\mathbf{x})) d\mathbf{x} \tag{9}$$

with $f = \chi(\gamma_i)$. Therefore, we consider the variation of W with respect to the components of the exponential coordinates[1] ξ_i of the group $g_i = e^{\widehat{\xi_i}}$

$$\frac{\partial W}{\partial \xi_i} = \frac{\partial}{\partial \xi_i} \int_{\bar{\mu}} f(g(\mathbf{x})) d\mathbf{x} \tag{10}$$

$$= \int_{\bar{\mu}} \nabla f(g(\mathbf{x})) \frac{\partial}{\partial \xi_i} g(\mathbf{x}) d\mathbf{x}. \tag{11}$$

Using Green's theorem it is possible to write the variation as an integral along the contour of μ and one over $g(\bar{\mu})$ with a divergence integrand

$$\frac{\partial W}{\partial \xi_i}(g) = \int_{\mu} f(g(x)) \left\langle \frac{\partial}{\partial \xi_i} g(x), g^* N \right\rangle d\,s - \int_{g(\bar{\mu})} f(y) \nabla_y \cdot \left(\frac{\partial}{\partial \xi_i} g(g^{-1}(y)) \right) d\,y. \tag{12}$$

Therefore, the derivative with respect of the group action is

$$\frac{\partial \phi}{\partial \xi_i} = \int_{\bar{\mu} \cap g_i^{-1}(\gamma_i)} \left\langle \frac{\partial}{\partial \xi_i} g_i(x), g_i^* N_i \right\rangle d\,s. \tag{13}$$

Where N is the normal vector field to the boundary of $g_i^{-1}(\gamma_i)$ and g_i^* is the push forward induced by the map g_i. Detailed calculations are reported in Appendix A.

---

[1] Every finite-dimensional Lie group admits exponential coordinates. For the simple case of the isometries of the plane, the exponential coordinates can be computed in closed-form using Rodrigues' formula.

3.4 Evolution equations

Within the level set framework, a function ψ is evolved instead of the contour μ. The function ψ is negative inside μ, positive outside and zero on the contour. The evolution of ψ depends on the velocity of μ via the Hamilton-Jacobi equation

$$
\begin{cases}
u_t + \left(\alpha - \sum_{i=1}^{k} \chi(g_i^{-1}\gamma_i)\right)|\nabla u| = 0, \\
u(0,x) = \psi^{(t)}(x).
\end{cases}
\tag{14}
$$

The evolution equations follow

$$
\psi^{(t+1)}(x) = u(1, x\,|\psi^{(t)}) \tag{15}
$$

$$
\bar{\mu}^{(t)} = \{x : \psi(x) < 0\} \tag{16}
$$

$$
\xi_i^{(t+1)} = \xi_i^{(t)} - \beta_\xi \int_{\bar{\mu} \cap g_i^{-1}(\gamma_i)} \left\langle \frac{\partial}{\partial \xi_i} g_i(x), g_i^* N_i \right\rangle ds \tag{17}
$$

where β_ξ is a step parameter and $u(\cdot, \cdot\,|\psi^{(t)})$ is the solution of (14) with initial condition $u(0,x) = \psi^{(t)}(x)$.

3.5 Generalization to graylevel images

There are many possible generalizations of the above formulas. Here we present the case of gray level images. The case of color images is very similar so the equations will not be stated. The main idea is to work with a generic level set between the minimum and the maximum intensity levels and write the functional to match all the level sets *simultaneously* using the partial differential equation in Eq. (25). To derive this equation, let k images of the same object I_i, $i = 1, \ldots, k$ be given and

$$
\bar{\gamma}_i^\delta = \{x : I_i < \delta\} \tag{18}
$$

be the generic δ-underlevel of I_i, where δ is a positive constant. Then let

$$
\mu : \mathbb{R}^2 \to \mathbb{R} \tag{19}
$$

be a function that represents the complete image intensity (the choice of the name μ is not casual, since this will turn out to be the complete shape for the case of greylevel images) and

$$
\begin{aligned}
\bar{\mu}^\delta &= \{x : \mu < \delta\} \\
\mu^\delta &= \partial\bar{\mu}^\delta
\end{aligned}
\tag{20}
$$

respectively its underlevel and the boundary of the underlevel. From the same considerations developed for the case of a contour, we write the functional ϕ as

$$
\phi = \sum_{i=1}^{k} \sum_{j=1}^{n} A(\bar{\gamma}_i^\delta \setminus g_i(\bar{\mu}^j)) + \alpha \sum_{j=1}^{n} A(\mu^j) \tag{21}
$$

where j is a discretization of the level set δ

$$\phi = \sum_{i=1}^{k} \sum_{j=1}^{n} \int \chi(\gamma_i^\delta)(1 - \chi(g_i \mu^j)) d\mathbf{x} + \alpha \sum_{j=1}^{n} \int \chi(\mu^j) d\mathbf{x} \qquad (22)$$

and in the same way the derivatives of the functional can be obtained as

$$\frac{\partial \mu^j}{\partial t} = \left(\alpha - \sum_{i=1}^{k} \chi(g_i^{-1} \gamma_i^\delta) \right) N^j, \qquad (23)$$

$$\frac{\partial \phi}{\partial \xi_i} = - \sum_{j=1}^{n} \int_{\bar{\mu}^j \cap g_i^{-1}(\gamma_i^\delta)} \left\langle \frac{\partial}{\partial \xi_i} g_i(x), g_i^* N_i^\delta \right\rangle d s. \qquad (24)$$

After letting j go to the limit, Eq. (23) gives the Hamilton-Jacobi equation for the function μ:

$$\mu_t(t, x) + \left(\sum_{i=1}^{k} H\left(I_i(g_i(x)) - \mu(t, x)\right) - \alpha \right) |\nabla \mu(t, x)| = 0 \qquad (25)$$

where

$$H(s) = \begin{cases} 1 & \text{if } s > 0, \\ 0 & \text{if } s \le 0. \end{cases} \qquad (26)$$

Therefore, the evolution equation for both the function μ and the parameters g_i is given by

$$\begin{cases} \mu^{(t+1)}(x) = \mu^{(t)}(x) - \beta_\mu \left(\sum_{i=1}^{k} H\left(I_i(g_i^{(t)}(x)) - \mu^{(t)}(x)\right) - \alpha \right) |\nabla \mu^{(t)}(x)| \\ \xi_i^{(t+1)} = \xi_i^{(t)} - \beta_\xi \int H\left(I_i(g_i^{(t)}) - \mu^{(t)}\right) \left\langle \frac{\partial g_i^{(t)}}{\partial \xi_i^{(t)}}, (\nabla \gamma_i)(g_i^{(t)}(x)) \right\rangle dx \end{cases}$$

$$(27)$$

where β_μ and β_ξ are step parameters.

4 Experiments

A numerical implementation of the evolution equations (15),(16),(17) has been written within the level set framework proposed by Osher and Sethian [23] using an ultra narrow band algorithm and an alternating minimization scheme. A set of common shapes (hands, leaves, mice, letters) has been chosen and converted into binary images of 256×256 pixels. For each image of this set, a group of binary images with missing parts and with different poses has been generated (Figures 2, 4 curves $\gamma_1, \ldots, \gamma_5$).

The following level set evolution equation has been used

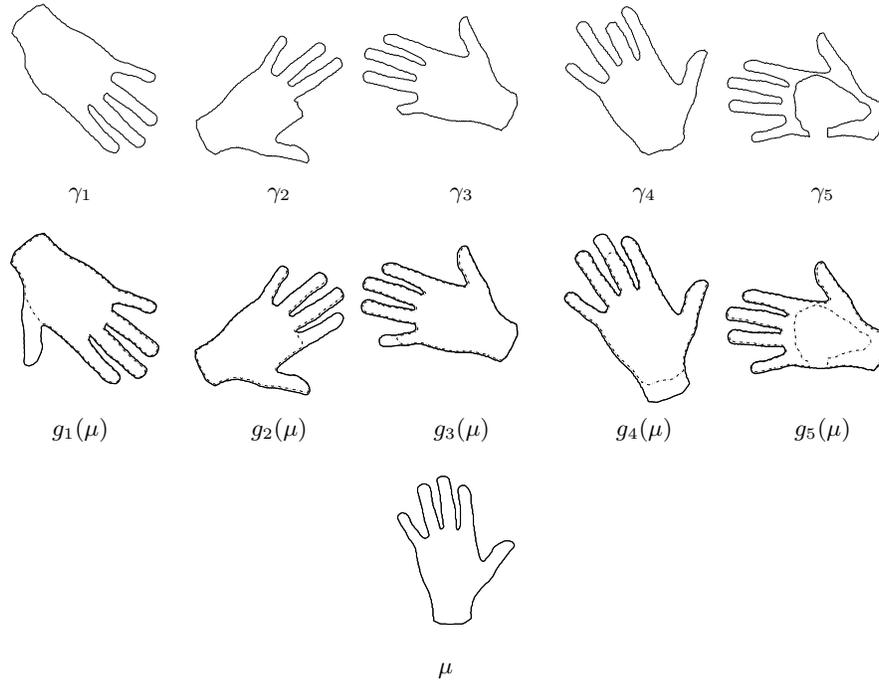$$\mu_t + \left(\alpha - \sum_{i=1}^{k} \chi(g_i^{-1} \gamma_i) \right) |\nabla \mu| = 0 \qquad (28)$$

Fig. 2. Hands. *(Top) a collection of images of the same hand in different poses with different missing parts. The support of the missing parts is unknown. (Middle) similarity group, visualized as a "registered" image. (Bottom) estimated template corresponding to the similarity group ("complete shape").*

with a first-order central scheme approximation. The evolution of the pose parameters has been carried out using the integral (17) with the following approximation of the arclength ds

$$ds \approx |\nabla(\mu)|d\mathbf{x}. \tag{29}$$

The evolution has been initialized with the following settings

$$\begin{aligned}
\mu_{t=0} &= \gamma_1 \\
T_i &= B_{\gamma_i} - B_{\gamma_1} \\
R_i &= \begin{pmatrix} \cos\theta_i & -\sin\theta_i \\ \sin\theta_i & \cos\theta_i \end{pmatrix}, \quad \text{with} \ \ \theta_i = \widehat{E_{\gamma_i} O E_{\gamma_1}}
\end{aligned} \tag{30}$$

where B_{γ_i} is the baricenter of γ_i and E_{γ_i} is the principal axis of inertia of the region $\bar{\gamma}_i$. The value of α has been set between 0 and 1. R_i, T_i are the rotational and translational components of $g_i = (R_i, T_i) \in SE(2)$.

In Figures 2, 4 some results have been illustrated. γ_j are the starting curves and μ is the complete shape in an absolute system after the computation. The figures show the computed $g_j(\mu)$, the estimated rigid motions.
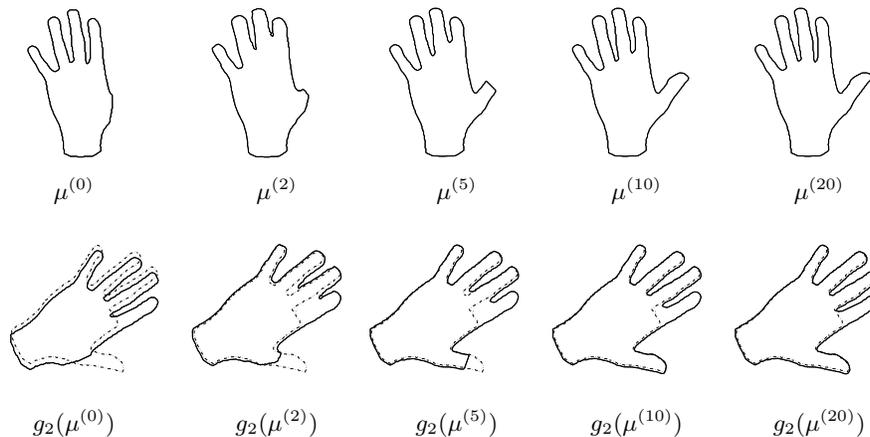
$$\mu^{(0)} \qquad \mu^{(2)} \qquad \mu^{(5)} \qquad \mu^{(10)} \qquad \mu^{(20)}$$

$$g_2(\mu^{(0)}) \qquad g_2(\mu^{(2)}) \qquad g_2(\mu^{(5)}) \qquad g_2(\mu^{(10)}) \qquad g_2(\mu^{(20)})$$

Fig. 3. Hands Evolution. *(Top) evolution of the complete shape for $t = 0, \ldots, 20$. (Bottom) evolution of $g_2(\mu)$ for $t = 0, \ldots, 20$.*

Figure 6 shows the method applied to grayscale images of a face, where different portions have been purposefully erased.

Figure 8 shows the results of matching a collection of images of the corpus callosum of a patient. One way to further improve this technique is to use richer finite-dimensional groups G that can account for more than simple rotations and translations. Simple examples include the affine and projective groups, for which the derivation is essentially the same, except for a few changes of measure due to the fact that they are not isometric.

The experiments show that this method works very well even when the missing part in each image is pretty significant, up to about 20% of the area.

References

1. R. Azencott, F. Coldefy, and L. Younes. A distance for elastic matching in object recognition. *Proc. 13th Intl. Conf. on Patt. Recog*, 1:687–691, 1996.

2. S. Belongie, J. Malik, and J. Puzicha. Matching shapes. In *Proc. of the IEEE Intl. Conf. on Computer Vision*, 2001.

3. D. Bereziat, I. Herlin, and L. Younes. Motion detection in meteorological images sequences: Two methods and their comparison. In *Proc. of the SPIE*, 1997.

4. M. Berger and G. Gerig. Deformable area-based template matching with application to low contrast imagery, 1998.

5. M. Burl, T. Leung, and P. Perona. Face localization via shape statistics. In *Proc. Intl. Workshop on automatic face and gesture recognition*, pages 154–159, Zurich, June 1995. IEEE Computer Soc.

6. T. K. Carne. The geometry of shape spaces. *Proc. of the London Math. Soc. (3) 61*, 3(61):407–432, 1990.

7. H. Chui and A. Rangarajan. A new algorithm for non-rigid point matching. In *Proc. of the IEEE Intl. Conf. on Comp. Vis. and Patt. Recog.*, pages 44–51, 2000.
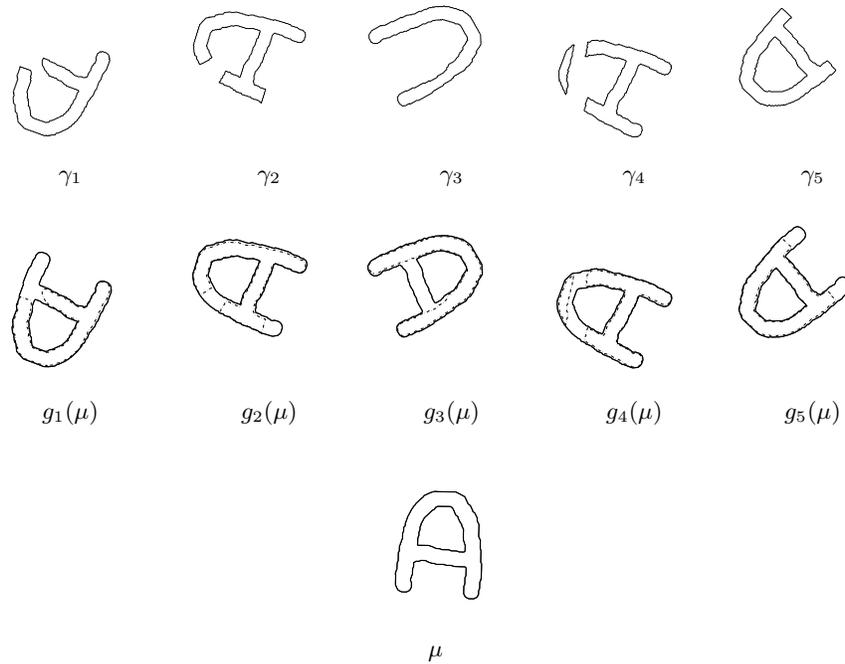
Fig. 4. Letter "A." *(Top) a collection of images of the letter "A" in different poses with different missing parts. The support of the missing parts is unknown. (Middle) similarity group ("registration"). (Bottom) estimated template corresponding to the similarity group ("complete shape").*

8. M. Fischler and R. Elschlager. The representation and matching of pictorial structures. *IEEE Transactions on Computers*, 22(1):67–92, 1973.

9. U. Grenander. *General Pattern Theory*. Oxford University Press, 1993.

10. U. Grenander and M. I. Miller. Representation of knowledge in complex systems. *J. Roy. Statist. Soc. Ser. B*, 56:549–603, 1994.

11. S. H. Kang, T. F. Chan, and S. Soatto. Multiple image inpainting. In *Proc. of the 3DPVT*, Padova, IT, June 2002.

12. D. G. Kendall. Shape manifolds, procrustean metrics and complex projective spaces. *Bull. London Math. Soc.*, 16, 1984.

13. B. Kimia, A. Tannebaum, and S. Zucker. Shapes, shocks, and deformations i: the components of two-dimensional shape and the reaction-diffusion space. *Int'l J. Computer Vision*, 15:189–224, 1995.

14. R. Kimmel and A. Bruckstein. Tracking level sets by level sets: a method for solving the shape from shading problem. *Computer Vision, Graphics and Image Understanding*, (62)1:47–58, 1995.

15. R. Kimmel, N. Kiryati, and A. M. Bruckstein. Multivalued distance maps for motion planning on surfaces with moving obstacles. *IEEE Trans. Robot. & Autom.*, 14(3):427–435, 1998.
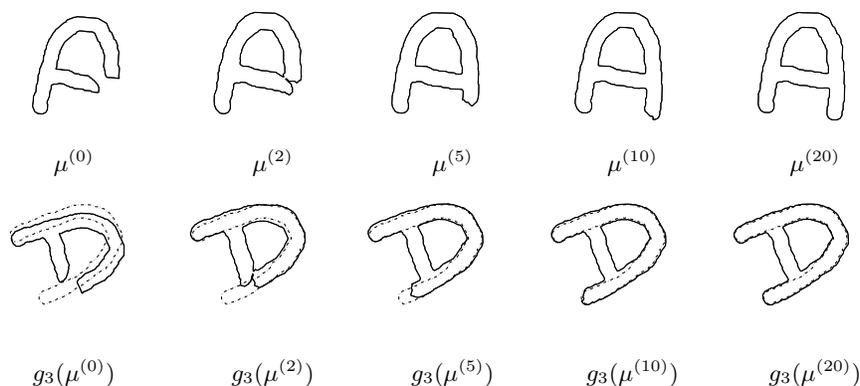
Fig. 5. Letter "A" Evolution. *(Top) evolution of the complete shape for* $t = 0, \ldots, 20$. *(Bottom) evolution of* $g_3(\mu)$ *for* $t = 0, \ldots, 20$.

16. M. Lades, C. Borbruggen, J. Buhmann, J. Lange, C. von der Malsburg, R. Wurtz, and W. Konen. Distortion invariatn object rcognition in the dynamic link architecture. *IEEE Trans. on Computers*, 42(3):300–311, 1993.

17. H. Le and D. G. Kendall. The riemannian structure of euclidean shape spaces: a novel environment for statistics. *The Annals of Statistics*, 21(3):1225–1271, 1993.

18. R. Malladi, R. Kimmel, D. Adalsteinsson, V. Caselles G. Sapiro, and J. A. Sethian. A geometric approach to segmentation and analysis of 3d medical images. In *Proc. Mathematical Methods in Biomedical Image Analysis Workshop*, pages 21–22, 1996.

19. R. Malladi, J. A. Sethian, and B. C. Vemuri. Shape modeling with front propagation: A level set approach. *IEEE Trans. on Pattern Analysis and Machine Intelligence*, 17(2):158–175, 1995.

20. K. V. Mardia and I. L. Dryden. Shape distributions for landmark data. *Adv. appl. prob.*, 21(4):742–755, 1989.

21. M. I. Miller and L. Younes. Group action, diffeomorphism and matching: a general framework. In *Proc. of SCTV*, 1999.

22. C. Nastar, B. Moghaddam, and A. Pentland. Generalized image matching: Statistical learning of physically-based deformations. In *Proceedings of the Fourth European Conference on Computer Vision (ECCV'96)*, Cambridge, UK, April 1996.

23. S. Osher and J. Sethian. Fronts propagating with curvature-dependent speed: algorithms based on hamilton-jacobi equations. *J. of Comp. Physics*, 79:12–49, 1988.

24. X. Pennec. Multiple Registration and Mean Rigid Shapes - Application to the 3D case. In I.L. Dryden K.V. Mardia, C.A. Gill, editor, *Image Fusion and Shape Variability Techniques (16th Leeds Annual Statistical (LASR) Workshop)*, pages 178–185, july 1996.

25. Anand Rangarajan, Haili Chui, and Eric Mjolsness. A new distance measure for non-rigid image matching. In *Energy Minimization Methods in Computer Vision and Pattern Recognition*, pages 237–252, 1999.

26. C. Samson, L. Blanc-Feraud, G. Aubert, and J. Zerubia. A level set model for image classification. In *in International Conference on Scale-Space Theories in Computer Vision*, pages 306–317, 1999.

27. K. Siddiqi, A. Shokoufandeh, S. Dickinson, and S. Zucker. Shock graphs and shape matching, 1998.
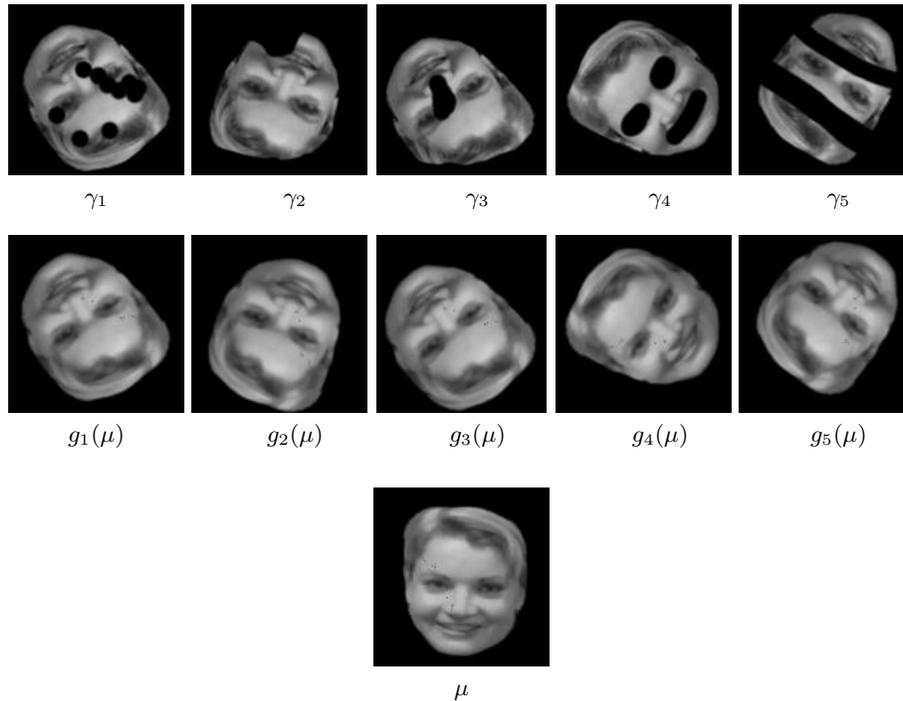
γ_1 γ_2 γ_3 γ_4 γ_5

$g_1(\mu)$ $g_2(\mu)$ $g_3(\mu)$ $g_4(\mu)$ $g_5(\mu)$

μ

Fig. 6. Faces *(Top) a collection of images of the same face in different poses with different missing parts. The support of the missing parts is unknown. (Middle) similarity group, visualized as a "registered" image. (Bottom) estimated template corresponding to the similarity group ("complete image").*

28. P. Thompson and A. W. Toga. A surface-based technique for warping three-dimensional images of the brain. *IEEE Trans. Med. Imaging*, 15(4):402–417, 1996.

29. R. C. Veltkamp and M. Hagedoorn. State of the art in shape matching. Technical Report UU-CS-1999-27, University of Utrecht, 1999.

30. A. Yezzi and S. Soatto. Stereoscopic segmentation. In *Proc. of the Intl. Conf. on Computer Vision*, pages 59–66, 2001.

31. L. Younes. Computable elastic distances between shapes. *SIAM J. of Appl. Math.*, 1998.

32. A. Yuille. Deformable templates for face recognition. *J. of Cognitive Neurosci.*, 3(1):59–70, 1991.

33. S. Zhu, T. Lee, and A. Yuille. Region competition: Unifying snakes, region growing, energy /bayes/mdl for multi-band image segmentation. In *Int. Conf. on Computer Vision*, pages 416–423, 1995.
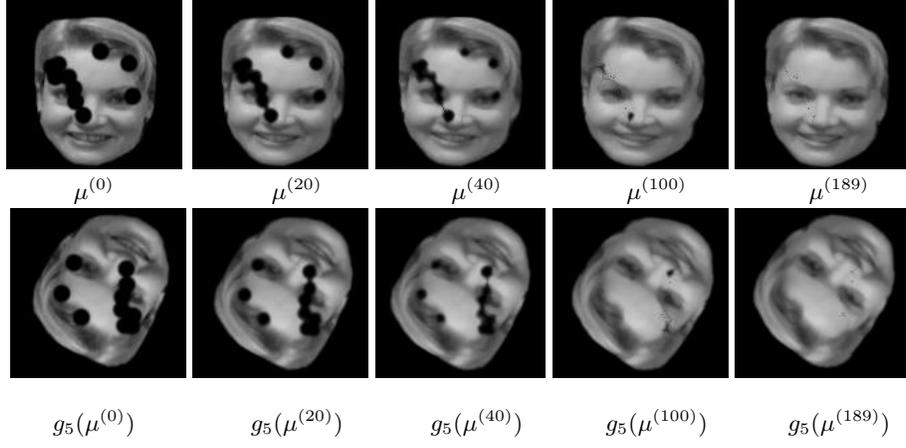
Fig. 7. Face evolution. *(Top) evolution of the complete image for* $t = 0, \ldots, 189$. *(Bottom) evolution of* $g_5(\mu)$ *for* $t = 0, \ldots, 189$.

A   Group action derivation details

$$
\begin{aligned}
\frac{\partial W}{\partial \xi_i} &= \int_{\bar{\mu}} \nabla f(g(\mathbf{x})) \frac{\partial}{\partial \xi_i} g(\mathbf{x}) d\,x = \int_{g(\bar{\mu})} \nabla f(y) \frac{\partial}{\partial \xi_i} g(g^{-1}(y)) d\,y \\
&= \int_{\partial g(\bar{\mu})} f(y) \left\langle \frac{\partial}{\partial \xi_i} g(g^{-1}(y)), N \right\rangle d\,s - \int_{g(\bar{\mu})} f(y) \nabla_y \cdot \left(\frac{\partial}{\partial \xi_i} g(g^{-1}(y)) \right) d\,y \\
&= \int_{\mu} f(g(x)) \left\langle \frac{\partial}{\partial \xi_i} g(x), g^* N \right\rangle d\,s + \int_{g(\bar{\mu}) \cap \bar{\gamma}_i} \nabla_y \cdot \left(\frac{\partial}{\partial \xi_i} g(g^{-1}(y)) \right) d\,y \\
&= -\int_{\mu \cap g^{-1}(\bar{\gamma}_i)} \left\langle \frac{\partial}{\partial \xi_i} g(x), g^* N \right\rangle d\,s + \int_{\partial(\bar{\mu} \cap g^{-1}(\bar{\gamma}_i))} \left\langle \frac{\partial}{\partial \xi_i} g(x), g^* N \right\rangle d\,s \\
&= \int_{\bar{\mu} \cap g^{-1}(\gamma_i)} \left\langle \frac{\partial}{\partial \xi_i} g(x), g^* N \right\rangle d\,s
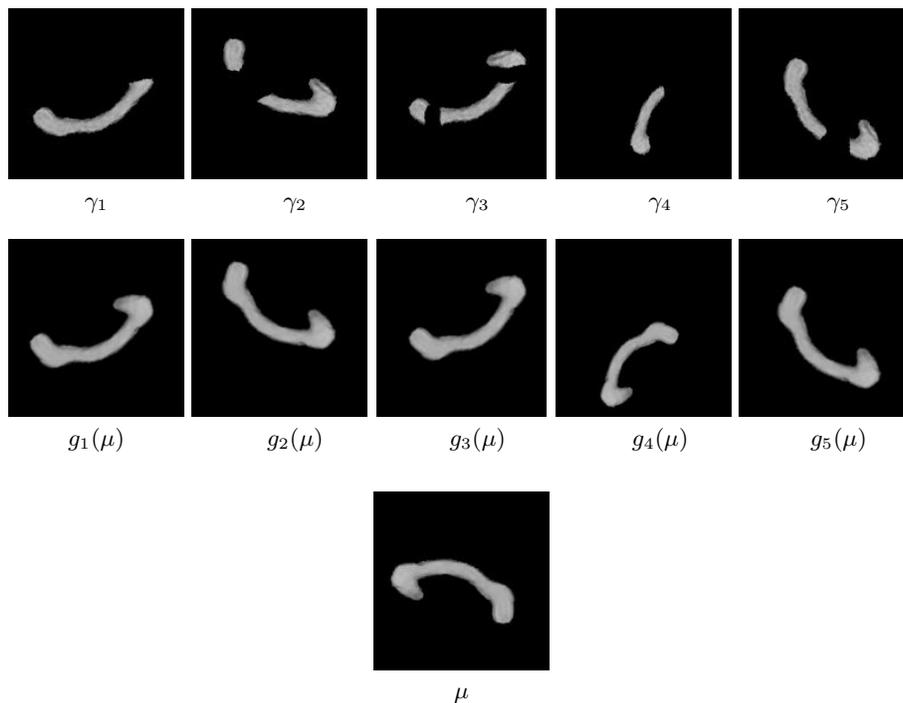\end{aligned}
$$

Fig. 8. Corpus Callosum. *(Top) a collection of images of the same corpus callosum in different poses with different missing parts. The support of the missing parts is unknown. (Middle) similarity group, visualized as a "registered" image. (Bottom) estimated template corresponding to the similarity group ("complete image").*
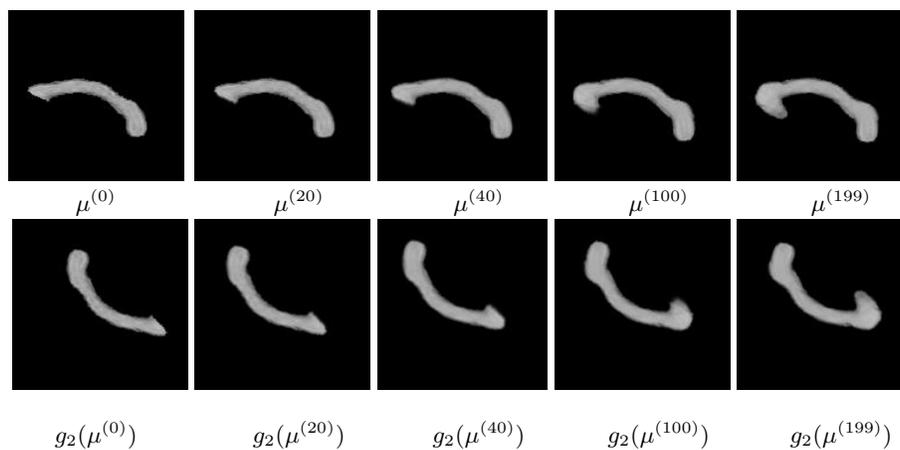

Fig. 9. Corpus Callosum evolution. *(Top) evolution of the complete image for $t = 0, \ldots, 199$. (Bottom) evolution of $g_2(\mu)$ for $t = 0, \ldots, 199$.*